



### **Science Arts & Métiers (SAM)**

is an open access repository that collects the work of Arts et Métiers Institute of Technology researchers and makes it freely available over the web where possible.

This is an author-deposited version published in: <https://sam.ensam.eu>  
Handle ID: <http://hdl.handle.net/10985/17725>

#### **To cite this version :**

Jerome BUIRE, Frédéric COLAS, Jean-Yves DIEULOT, Leticia DE ALVARO, Xavier GUILLAUD -  
Confidence Level Optimization of DG Piecewise Affine Controllers in Distribution Grids - IEEE  
Transactions on Smart Grid - Vol. 10, n°6, p.6126-6136 - 2019

Any correspondence concerning this service should be sent to the repository

Administrator : [scienceouverte@ensam.eu](mailto:scienceouverte@ensam.eu)





### **Science Arts & Métiers (SAM)**

is an open access repository that collects the work of Arts et Métiers ParisTech researchers and makes it freely available over the web where possible.

This is an author-deposited version published in: <https://sam.ensam.eu>  
Handle ID: <http://hdl.handle.net/null>

#### **To cite this version :**

Jerome BUIRE, Frederic COLAS, Jean-Yves DIEULOT, Leticia DE ALVARO, Xavier GUILLAUD -  
Confidence Level Optimization of DG Piecewise Affine Controllers in Distribution Grids - IEEE  
Transactions on Smart Grid - Vol. 10, n°6, p.6126-6136 - 2019

Any correspondence concerning this service should be sent to the repository

Administrator : [archiveouverte@ensam.eu](mailto:archiveouverte@ensam.eu)



# Confidence level optimization of DG piecewise affine controllers in distribution grids

Jérôme Buire, *Student Member, IEEE*, Frédéric Colas, Jean-Yves Dieulot, Leticia De Alvaro, Xavier Guillaud, *Member, IEEE*

**Abstract**—Distributed generators (DG) reactive powers are controlled to mitigate voltage overshoots in distribution grids with stochastic power production and consumption. Classical DGs controllers may embed piecewise affine laws with dead-band terms. Their settings are usually tuned using a decentralized method which uses local data and optimizes only the DG node behavior. It is shown that when short-term forecasts of stochastic powers are Gaussian and the grid model is assumed to be linear, nodes voltages can either be approximated by Gaussian or sums of truncated Gaussian variables. In the latter case, the voltages probability density functions (pdf) that are needed to compute the overvoltage risks or DG control effort are less straightforward than for normal distributions. These pdf are used into a centralized optimization problem which tunes all DGs control parameters. The objectives consist of maximizing the confidence levels for which voltages and powers remain in prescribed domains and minimizing voltage variances and DG efforts. Simulations on a real distribution grid model show that the truncated Gaussian representation is relevant and that control parameters can easily be updated even when extra DGs are added to the grid. **The DG reactive power** can be reduced up to 50 % or node voltages variances can be reduced up to 30 %.

**Index Terms**—Confidence level optimization; control tuning; distribution network; piecewise affine controller; stochastic power flow.

## NOMENCLATURE AND ACRONYMS

DG	Distributed Generator.
OLTC	On Load Tap Changer.
HV, MV	High voltage, Medium voltage.
$n + 1, m$	Number of nodes, number of DGs
$\mathbb{I}$	Vector of 1s, dimension $n$ .
$\tilde{\mathbf{V}}$	Vector of voltages, nodes 1 to $n$ : $\tilde{\mathbf{V}} = [\tilde{V}_1, \dots, \tilde{V}_n]^T$ .
$\tilde{V}_0$	OLTC node voltage.
$V_0^{ref}$	OLTC node voltage reference.
$V_0^{err}$	OLTC node voltage error.
$\tilde{\mathbf{I}}$	Vector of currents entering or exiting nodes ( $\tilde{\mathbf{I}} = [\tilde{I}_1, \dots, \tilde{I}_n]^T$ ).
$\tilde{I}_0$	Currents entering or exiting slack bus 0.
$\mathbf{Y}$	Admittance matrix.
$\mathbf{Z}$	Impedance matrix, $\mathbf{Z} = \mathbf{Y}^{-1}$ .

$\tilde{\mathbf{P}}$	vector of active powers ( $\tilde{\mathbf{P}} = [\tilde{P}_1, \dots, \tilde{P}_n]^T$ ).
$\tilde{\mathbf{P}}^l$	vector of consumption active powers ( $\tilde{\mathbf{P}}^l = [\tilde{P}_1^l, \dots, \tilde{P}_n^l]^T$ ).
$\tilde{\mathbf{P}}^p$	Vector of production reactive powers ( $\tilde{\mathbf{P}}^p = [\tilde{P}_1^p, \dots, \tilde{P}_n^p]^T$ ).
$\tilde{\mathbf{Q}}$	Vector of reactive powers ( $\tilde{\mathbf{Q}} = [\tilde{Q}_1, \dots, \tilde{Q}_n]^T$ ).
$\tilde{\mathbf{Q}}^l$	Vector of consumption reactive powers ( $\tilde{\mathbf{Q}}^l = [\tilde{Q}_1^l, \dots, \tilde{Q}_n^l]^T$ ).
$\tilde{\mathbf{Q}}^p$	List of production reactive powers ( $\tilde{\mathbf{Q}}^p = [\tilde{Q}_1^p, \dots, \tilde{Q}_n^p]^T$ ).
$Q_i^{shunt}$	Reactive power of node $i$ shunt admittance.
$P_i^N$	DG nominal power at node $i$ .
$\alpha, \beta, Q^0$	Control parameters vectors of affine or piecewise affine laws.
$\gamma$	Breakpoints vector of piecewise affine control laws.
$a_i, b_i$	Vector of truncations at voltage $V_i$ .
$\mu_{\tilde{X}}, \sigma_{\tilde{X}}$	Mean and standard deviation of the stochastic variable $\tilde{X}$ .
$\mathcal{N}(\mu, \sigma^2)$	Normal distribution with mean $\mu$ and variance $\sigma^2$ .
$TN(\mu, \sigma^2, a, b)$	Normal distribution with mean $\mu$ and variance $\sigma^2$ truncated in the interval $[a, b]$ .
$x \mapsto \phi(x)$	Standard Gaussian probabilistic distribution function.
$x \mapsto \Phi(x)$	Standard Gaussian cumulative distribution function.
$\chi^2$	Pearson's chi-squared test.
$w_V, w_Q$	Objective function weighting factors.
$\eta, \lambda$	Confidence levels.

## I. INTRODUCTION

WITH a high penetration level of renewable energy generation, distribution grids face new issues such as reverse power flows. Consequently, the likelihood of voltage violations of the prescribed domain (mainly over-voltage situations) is increased [1]. The magnitude and location of these voltage violations depend on the network topology and on the uncontrollable stochastic inputs (i.e. the active power of DGs and the power consumption of loads); however, they can be mitigated by controlling the On Load Tap Changer (OLTC) voltage reference and the Distributed Generators (DGs) reactive powers. Because these controllers embed only local

Manuscript received september 06, 2018; revised december 01, 2018.

J. Buire, F. Colas and X. Guillaud are with Univ. Lille, Arts et Metiers ParisTech, Centrale Lille, HEI, EA 2697 - L2EP - Laboratoire d'Electrotechnique et d'Electronique de Puissance, F-59000, Lille, France (e-mail: jerome.buire@centralelille.fr; frederic.colas@ensam.eu xavier.guillaud@centralelille.fr).

J.Y. Dieulot is with Univ. Lille, CNRS, Centrale Lille, UMR 9189 - CRISTAL - Centre de Recherche en Informatique Signal et Automatique de Lille, F-59000 Lille, France (e-mail: Jean-Yves.dieulot@polytech-lille.fr).

L. De Alvaro is with Enedis, F-92079 Paris-La-Defense, France (e-mail: leticia.de-alvaro@enedis.fr).

measurements, the system is communication fault tolerant and each controller can operate in standalone mode (with intermittent or without communication) [2]. These controllers have a simple structure and do not need to be optimized in real-time (as for Model Predictive Controllers proposed in [3], [4]).

The main problem addressed by this paper is the centralized tuning of local controllers' parameters, under intermittent power production and consumption, using a stochastic approach. As discussed in the survey [5], most existing methods proposed to tune volt/var curves are based on deterministic approaches which often consider worst-case bounds to cope with uncertainties. These bounds neither consider the production and consumption patterns which are very different according to the seasons, the day of the week, the hours, etc., nor the many interactions between the grid components of a real distribution network (loads, DGs, conductors). The use of error bounds tuning methods may yield very conservative solutions and generate a significant control effort to keep the voltages within prescribed values. When a high number of DGs with intermittent production are connected to the grid, it is recommended to use an intraday centralized control parameters tuning method to save reactive power. Such a daily scheduling algorithm is improved when the random nature and stochastic characteristics of the power production and power consumption day-ahead forecasts are taken into account because it is possible to estimate the probabilities that the grid operates according to the European regulations.

An important contribution of the paper is to propose a model that is able to provide the stochastic profiles of each node voltage and an estimate of the likelihood of voltage violation. Another contribution consists of using a confidence level optimization method which minimizes the violation risks and which is not found in the literature. Quantile optimization requires to find the maximum bound  $V_{max}$  such that the probability that voltages are smaller than  $V_{max}$  is greater than a fixed confidence level  $p$  (e.g. 0.95) [6]. On the other hand, confidence level optimization aims to maximize  $p$  when  $V_{max}$  is given, that is find the minimum possible risk (here of voltage overvoltage). In the power system literature, adjusting or minimizing the confidence level has been done so far only for Unit Commitment or pricing problems [7], [8], but has not addressed control parameter tuning. In general, confidence level optimization are not convex [9], and chance-constrained relaxation as Chebychev generating functions [10] are not applicable.

A main benefit over robust optimization algorithms, which update control parameters using uncertainty bounds regardless of the load and the production forecasting stochastic distributions [11], [12] is that these methods are able to provide confidence levels, that is a rate of service for the DSO or the customers. Moreover, the representation given in this paper is a stochastic extension of an accurate linear model of [13] which allows the use of convex optimization, provides the probability distribution of each node voltage and greatly alleviates the computational time. The computational time issue is quite important as the optimization algorithm should perform hourly updates. Contrary to the algorithm presented in the paper, most

stochastic methods for power systems that are found in the literature are based on sampling and a nonlinear model of the grid such as the well-known Monte-Carlo Simulation (MCS). Such methods should be discarded, because they bear a significant computational burden - at least a few hours - for large scale grids [14], even with the use of relaxation techniques [15], [16],

In practice, a local industrial controller embeds a nonlinear dead-band term, which alleviates unnecessary reactive power actuation, and saturations. More generally, the literature considers smooth linear or nonlinear droop controllers and ignores centralized tuning methods that can be applied on real size networks which embed piecewise affine control laws [12] (with the exception of [17] which displays a scenario without any stochastic variables). An original contribution of the paper is to find easily the probability densities and confidence levels of node voltages generated by the use of piecewise affine controllers and to tune optimally the breakpoints and dead-band width.

In this paper, the DG reactive power control parameters are optimized using a stochastic centralized approach with a low computational time for real size networks. This stochastic approach realizes a trade-off between voltage variances, DG control effort, and confidence levels that voltages and powers remain within prescribed domains, which is not covered by the literature. Moreover, a precise stochastic representation of the grid is given when some of the DG have a piecewise affine reactive power control law (e.g. droop control with a deadband) and using the stochastic characteristics of the production and consumption forecasts considered. It is shown that the node voltages can be represented either by Gaussian or sums of truncated Gaussian distributions. The existence of such distributions assumes that the error of the daily short-term forecast of consumption and production can be characterized by Gaussian distributions, as highlighted in [18], along with an accurate linear power flow model such as found in [13]. This stochastic truncated law has only been used to characterize the production or consumption powers in the literature [19], [20] and not the node voltages. This allows, in real-time, to compute means, variances, confidence levels, etc. and to perform the confidence level optimization of the grid. While keeping the industrial control structure, the main benefits of the methodology are the computation and optimization of confidence levels (i.e. rates of service) at a reasonable control cost.

The paper is organized as follows: In section II, the linear stochastic power flow, the stochastic modeling of inputs and the controller structure are presented. Section III introduces truncated Gaussian distributions, the optimization problem and the procedure to solve it. A simulation of a real distribution grid is given in section IV.

## II. STOCHASTIC MODELING OF THE SYSTEM

### A. Linear power flow model

In this section, accurate linear models are presented which introduce the nodes voltages ( $\tilde{\mathbf{V}}$ ) as linear functions of load/production active ( $\tilde{\mathbf{P}}$ ) and reactive ( $\tilde{\mathbf{Q}}$ ) powers [13], [21] which is briefly recalled hereafter. Bold variables represent

matrices or vectors. A tilde ( $\tilde{\cdot}$ ) placed on top of a symbol indicates that the corresponding variable is stochastic. The subscript  $i$  refers to node  $i$ . Subscript is  $g$  for a node which contains a generator. Superscript refers to some property of the variable. For example, superscript  $j$  refers to the  $j^{th}$  interval of the piecewise affine control law.

We consider a distribution grid comprising some lines, loads,  $n+1$  nodes and  $m$  DGs. The slack bus 0 has a voltage ( $\tilde{V}_0$ ) and a zero angle. It refers to the secondary of the HV/MV distribution transformer and is controlled by an On Load Tap Changer (OLTC). Tap changer is a mechanism in transformers which allows for variable turn ratios to be selected in discrete steps [4]. Note that due to this intrinsic quantization, the precision of this actuator is around 1%. The other bus voltages are noted  $\tilde{\mathbf{V}} = [\tilde{V}_1, \dots, \tilde{V}_n]^T$ . The study is restricted to the steady state behavior of the system. All voltages and currents are sinusoidal signals which have the same frequency and can be represented as complex numbers. Ohm's and Kirchhoff's circuit laws establish relation (1), where  $\tilde{\mathbf{Y}}$  represent a known non stochastic admittance matrices:

$$\begin{bmatrix} \tilde{I}_0 \\ \tilde{\mathbf{I}} \end{bmatrix} = \mathbb{Y} \begin{bmatrix} \tilde{V}_0 \\ \tilde{\mathbf{V}} \end{bmatrix} = \begin{bmatrix} Y_0 & \mathbf{Y}_{0v} \\ \mathbf{Y}_{v0} & \mathbf{Y} \end{bmatrix} \begin{bmatrix} \tilde{V}_0 \\ \tilde{\mathbf{V}} \end{bmatrix} \quad (1)$$

Shunt admittances are neglected in this linear approximation [13]. However, in distribution networks, many underground cables can be found for which these shunt admittances cannot be neglected and are represented by capacitances  $Y_{ii}$ . In order to keep the model simple, they are considered as constant reactive power productions  $Q_i^{shunt}$  which are added to the power buses and computed assuming that the deterministic voltage value  $V_h$  has been fixed (typically we choose 1 pu):

$$Q_i^{shunt} = Y_{ii} V_h^2 \quad (2)$$

The linear approximation of the nodes voltages (3), for which  $\mathbf{Z} = \mathbf{Y}^{-1}$  and vectors  $\tilde{\mathbf{P}}$  and  $\tilde{\mathbf{Q}}$  are the sets of active and reactive powers, is valid under condition (4).

$$\tilde{\mathbf{V}} = \tilde{V}_0 (\mathbb{I} + \frac{1}{\tilde{V}_0^2} \mathbf{Z} (\tilde{\mathbf{P}} - j\tilde{\mathbf{Q}})) \quad (3)$$

$$\tilde{V}_0^2 > 4 \|\mathbf{Z}\|^* \|\tilde{\mathbf{P}} + j\tilde{\mathbf{Q}}\| \quad (4)$$

where the vector 2-norm  $\|\cdot\|$  on  $\mathbb{C}^N$  and the matrix norm  $\|\cdot\|^*$  are defined in (5) on  $\mathbb{C}^{N \times N}$ .

$$\|A\|^* = \max_h \|A_{h*}\| = \max_h \sqrt{\sum_k |A_{hk}|^2} \quad (5)$$

The theoretical upper bound of the voltage error at the node  $j$  is given by (6). Monte Carlo simulations of real distribution networks have shown that the real error is lower than 0.001 pu and far below the theoretical upper bound of the voltage error which is below 0.01 pu [22].

$$|\hat{\tilde{V}}_i - \tilde{V}_i| = \frac{4}{\tilde{V}_0^3} \|Z_{i*}\| \|\mathbf{Z}\| \quad (6)$$

Eventually, the linear power flow model is given by the generic equation (7), which will be used for next discussions.

$$\tilde{\mathbf{V}} = \mathbf{A}\tilde{\mathbf{P}} + \mathbf{B}\tilde{\mathbf{Q}} + \mathbb{I}\tilde{V}_0 \quad (7)$$

A simple estimation of current lines is obtained by the admittance matrix and Ohm's law.

## B. Stochastic modeling of inputs

The inputs (consumption and production powers) are characterized by their statistical properties and they come from day-ahead forecasts. The time-dependent power profile is not embedded in the control algorithm. Besides voltage expectations, the PDFs of voltages and confidence levels should be considered. This can be achieved using the linear model (7), stochastic forecasting data and model uncertainties. Let us split power vectors  $\tilde{\mathbf{P}}$  in (8) and  $\tilde{\mathbf{Q}}$  in (9) in consumptions  $\tilde{\mathbf{P}}^1$  and  $\tilde{\mathbf{Q}}^1$  and productions  $\tilde{\mathbf{P}}^P$  and  $\tilde{\mathbf{Q}}^P$  (the nominal power of the DG of the node  $i$  is noted  $P_i^N$ ).  $\tilde{\mathbf{P}}^1$  is a stochastic variable which is not used for feedback.  $\tilde{\mathbf{P}}^P$  corresponds to the DG stochastic active power which will not be curtailed in this paper but can be used in the feedback control law of the DG reactive power controllers. In this paper, the control variable is the reactive power

$$\tilde{\mathbf{P}} = \tilde{\mathbf{P}}^1 - \tilde{\mathbf{P}}^P \quad (8)$$

$$\tilde{\mathbf{Q}} = \tilde{\mathbf{Q}}^1 - \tilde{\mathbf{Q}}^P \quad (9)$$

Productions and consumptions are provided by short term forecasting [18], [23]. Fig.1 shows two examples of the short-term (e.g. daily) wind power forecasting error probability density functions (PDF); their histograms can be approximated by Gaussian distributions. Likewise, stochastic consumptions and productions powers can be modeled as Gaussian variables. The voltage  $\tilde{V}_0$  is controlled by the OLTC which selects the appropriate tap according to the voltage reference  $V_0^{ref}$  which is prescribed by the distribution transformer [4]. The absolute voltage error is limited by 0.01 pu.  $V_0$  can also be considered as a stochastic variable. Using historical data, the voltage error distribution can be approximated by a Gaussian law, in the case study  $\tilde{V}_0^{err} = \mathcal{N}(0, 0.05^2)$ . A Gaussian variable is completely characterized by its mean  $\mu$  and standard deviation  $\sigma$ .

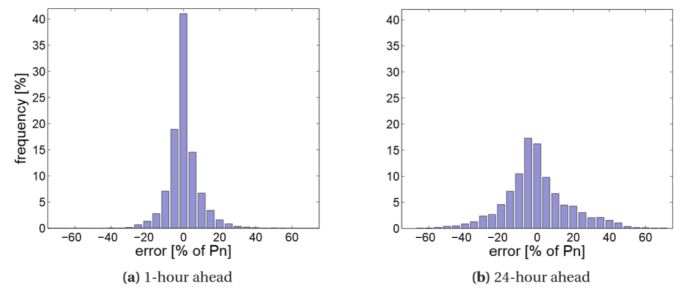


Fig. 1. Error of wind power forecasting [23]

As all variables which are fed to the linear model (7) are assumed to be Gaussian, it is possible to show that nodes voltages and powers are also Gaussian which means and standard deviations can be determined analytically without any iteration.

### C. Structure of local controllers

In distribution networks, the actuators are the OLTC and the distributed generators reactive powers. The voltage reference  $V_0^{ref}$  is the OLTC control parameter defined by (10) [4]:

$$\tilde{V}_0 = V_0^{ref} + \tilde{V}_0^{err} \quad (10)$$

The error voltage  $\tilde{V}_0^{err} = \mathcal{N}(0, 0.05^2)$  comes mainly from quantization (tap selection). Contrary to the OLTC, the DGs are scattered all over the distribution grid. The structure of the DG reactive power industrial controllers can be either affine or piecewise affine. In the first case, the reactive power is an affine function of local measurements such as the voltage and the active power production. The affine controller of a DG located at the node  $g$  is given by equation (11).

$$\tilde{Q}_k^p = \alpha_k \tilde{V}_k + \beta_k \tilde{P}_k^p + Q_k^0 \quad (11)$$

$\tilde{P}_k^p$  and  $\tilde{V}_k$  are respectively the active power production and the voltage of the node  $k$ .  $\alpha_k$ ,  $\beta_k$  and  $Q_k^0$  are the controller parameters.

In the second case, the continuous control law is piecewise affine and uses only local voltage feedback. The common industrial practice is 5 intervals, and displays two affine sections, two saturation levels, and a deadband [24]. The levels and breakpoints extremal values are chosen in order to guarantee the system stability and to keep the control within the regulatory requirements (PQ diagrams). Without loss of generality, this work can be extended to any piecewise affine control law. The piecewise affine control law at the node  $g$  is given by equation (12) [24].

$$\tilde{Q}_g^p = \begin{cases} \alpha_g^1 \tilde{V}_g + Q_g^{01} & \text{if } \tilde{V}_g < \gamma_g^1 \\ \alpha_g^2 \tilde{V}_g + Q_g^{02} & \text{if } \gamma_g^1 \leq \tilde{V}_g < \gamma_g^2 \\ \alpha_g^3 \tilde{V}_g + Q_g^{03} & \text{if } \gamma_g^2 \leq \tilde{V}_g < \gamma_g^3 \\ \alpha_g^4 \tilde{V}_g + Q_g^{04} & \text{if } \gamma_g^3 \leq \tilde{V}_g < \gamma_g^4 \\ \alpha_g^5 \tilde{V}_g + Q_g^{05} & \text{if } \gamma_g^4 \leq \tilde{V}_g \end{cases} \quad (12)$$

$\tilde{V}_g$  is the voltage of the node  $g$ .  $\alpha_g^j$ ,  $Q_g^{0j}$  and  $\gamma_g^j$  are the controller parameters which are defined for each interval  $j$ , as shown in Fig. 2. **Deadbands prevent oscillations or repeated activation-deactivation cycles. Control saturation is necessary to avoid stability problems [24]. The controllable inputs are the DERs reactive powers. The main goal of the paper is to tune the parameters of the piecewise affine control laws which is described in the next section.**

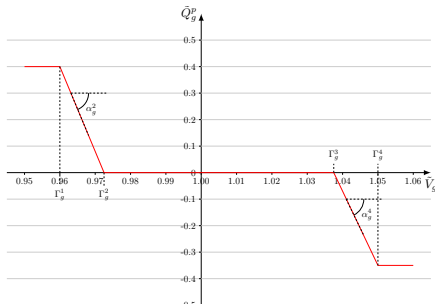


Fig. 2. Piecewise affine control law

### III. CONFIDENCE LEVEL OPTIMIZATION OF PIECEWISE AFFINE CONTROLLER PARAMETERS

In this section, it will be shown that stochastic laws of the nodes voltages of model (7) can be approximated by either Gaussian or sums of truncated Gaussian laws when the system is under piecewise affine control. Then, a confidence level optimization which embeds the voltages stochastic laws will determine the appropriate OLTC reference voltage and adjust the controller settings (levels and breakpoints) for each DG and for each interval.

#### A. Stochastic models of nodes voltages

Figure 3 shows the node voltages PDFs along a feeder embedding a single DG equipped with a piecewise affine controller located at its end. These profiles are obtained from a Monte Carlo simulation, assuming that the inputs are Gaussian. It can be noticed that when nodes are close to the OLTC, their voltages look like Gaussian variables, and when they are close to the DG, they behave as sums of truncated Gaussian variables ("TN" represents a truncated Gaussian variable which is detailed in the Appendix).

#### Proposition 1:

Consider a feeder with  $m$  nodes for which the voltage is controlled by a set of DG equipped with an affine controller defined in (11) and a single DG equipped with the piecewise affine reactive power control law defined in (12). Let  $\alpha^j$  a diagonal matrix for which the diagonal element  $\alpha_{ii}^j = \alpha_i$  when  $i$  is a linear DG node,  $\alpha_{ii}^j = 0$  when  $i$  is a load node, and  $\alpha_{ii}^j = \alpha_i^j$  corresponds to the slope of the piecewise affine control law of the DG node  $i$  for the interval  $j$ ,  $j = 1 \dots 5$ . The vector of control parameters  $\mathbf{Q}^{0j}$  is defined in the same way. Assume that the OLTC voltage and powers inputs are Gaussian and that **the invertibility condition**  $\det(\mathbf{I} - \mathbf{B}\alpha^j) \neq 0$ ,  $j = 1 \dots 5$ , is fulfilled, then, the voltage  $\tilde{V}_i$  at node  $i$  is a sum of truncated Gaussian variables, which distribution is given by:

$$\tilde{V}_i = \sum_{j=1}^5 TN(\mu_i^j, (\sigma_i^j)^2, a_i^j, b_i^j) \quad (13)$$

The truncations of the DG node  $g$  are:

$$a_g = \{-\infty, \gamma_g^1, \gamma_g^2, \gamma_g^3, \gamma_g^4\}, \quad (14)$$

$$b_g = \{\gamma_g^1, \gamma_g^2, \gamma_g^3, \gamma_g^4, +\infty\} \quad (15)$$

and the truncations of the node  $i$  ( $i \neq g$ ) are:

$$a_i = \{-\infty, \tilde{V}_i | \tilde{V}_g = \gamma_g^1, \tilde{V}_i | \tilde{V}_g = \gamma_g^2, \tilde{V}_i | \tilde{V}_g = \gamma_g^3, \tilde{V}_i | \tilde{V}_g = \gamma_g^4\} \quad (16)$$

$$b_i = \{\tilde{V}_i | \tilde{V}_g = \gamma_g^1, \tilde{V}_i | \tilde{V}_g = \gamma_g^2, \tilde{V}_i | \tilde{V}_g = \gamma_g^3, \tilde{V}_i | \tilde{V}_g = \gamma_g^4, +\infty\} \quad (17)$$

where  $\tilde{V}_i | \tilde{V}_g = \gamma_g^j$  is the conditional random variable  $V_i$  given  $V_g = \gamma_g^j$ .

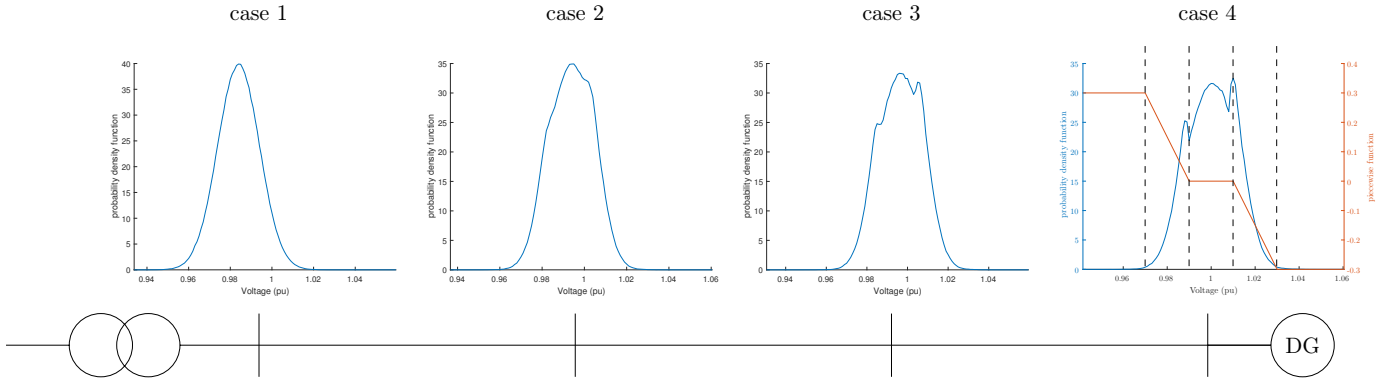


Fig. 3. Typical voltage profiles along a feeder

*Proof:* The linear power flow model (7) combined with equations (11, 12) yields the global piecewise linear model, equation (18).

$$\tilde{\mathbf{V}}^j = (\mathbf{I} - \mathbf{B}\alpha^j)^{-1}[(\mathbf{A} + \mathbf{B}\beta)\tilde{\mathbf{P}} + \mathbf{B}(\mathbf{Q}^{0j} + \mathbf{Q}^1) + \mathbb{I}\tilde{V}_0] \quad (18)$$

where  $\tilde{\mathbf{V}}^j$  refers to the nodes voltages within the interval  $j$  of the piecewise affine control law. As the inputs  $\tilde{\mathbf{P}}$  and  $\tilde{V}_0$  are Gaussian and the parameters  $\alpha^j$  and  $Q^{0j}$  are piecewise constant, each part of  $\tilde{\mathbf{V}}$  is a sum of weighted Gaussian so is Gaussian over each interval. However, the behavior at the DG node differs from that at the other nodes:

- The variable which triggers changes in the piecewise affine control law parameters, depending on the breakpoints ( $\gamma_g^1, \gamma_g^2, \gamma_g^3, \gamma_g^4$ ), is the DG node voltage. As a consequence, the DG node  $g$  is a sum of truncated Gaussian variables which intervals stem directly from the breakpoints (see Fig.3 case 4).
- For other nodes, which lie between the OLTC and the DG, the voltages given by equation (18) will always behave as Gaussian variables within each interval. However the truncations are not deterministic, because they depend on the stochastic behavior of the system. Indeed, the breakpoint  $\gamma_g^j$  of the DG node  $g$  propagated to the node  $i$  ( $i \neq g$ ) becomes the conditional random variable  $\tilde{V}_i | \tilde{V}_g = \gamma_g^j$ . Using the properties of multivariate conditional Gaussian variables [25], the stochastic truncation is a Gaussian variable which mean and variance are defined in (19, 20).

$$\mu_{\tilde{V}_i | \tilde{V}_g = \gamma_g^j} = \mu_{\tilde{V}_i} + \frac{CoV(\tilde{V}_i, \tilde{V}_g)}{\sigma_{\tilde{V}_g}^2} (\gamma_g^j - \mu_{\tilde{V}_g}) \quad (19)$$

$$\sigma_{\tilde{V}_i | \tilde{V}_g = \gamma_g^j}^2 = \sigma_{\tilde{V}_i}^2 + \frac{CoV(\tilde{V}_i, \tilde{V}_g)}{\sigma_{\tilde{V}_g}^2} CoV(\tilde{V}_g, \tilde{V}_i) \quad (20)$$

This second case is illustrated in Fig.3 case 2 and case 3.

Whereas Proposition 1 states that all node voltages can be represented by sums of truncated Gaussian variables, the main difficulty is to consider the stochastic truncations given by (16), (17). The computational effort required by the use of analytical tools allowing to take stochastic truncations into account (e.g. convolutions) is way too important for the

purpose of controller tuning. As a consequence, it is necessary to simplify the voltage stochastic model. Intuitively, two cases can be considered as shown in Fig. 3:

- When nodes are close to the DG (equipped with a piecewise affine controller), the stochastic truncations are narrow and boil down to their expectations. Hence, since the truncations are deterministic, the voltage distributions are approximated by sums of truncated Gaussian variables (case 3).
- When nodes are close to the OLTC (and far from the DG) the previous approximation does not hold any more and the truncated Gaussian PDFs, given by (18), have a substantial overlap. Hence, the node voltage behaves as a sum of many stochastic variables, and, by virtue of the Central Limit Theorem, converges to a Gaussian variable. Its characteristics are computed using a linearized control law and the global linear model in (18) (case 2).

There is no analytical method which allows to choose whether a node voltage distribution can be approximated either by a sum of piecewise Gaussian distributions or by a Gaussian distribution nor yields a quantitative bound for the approximation error. This selection is addressed in section III.B, using a chi-square test.

Remark: In the full affine control case (without any piecewise affine controller), the nodes voltages are completely defined by (18) and the Gaussian inputs; the nodes voltages are sums of Gaussian variables, and can therefore be defined by Gaussian variables [25]. Note also that the result of Proposition 1 is valid for one piecewise affine controller per feeder, but the number of other DGs with affine control is not restricted.

### B. Selection of the stochastic voltage model

Proposition 1 concludes on the fact that nodes voltages can be modeled either by Gaussian variables or sums of truncated Gaussian variables. **If the node voltages were modeled only by sums of truncated variables, one obtains 5 different truncated distributions for each node and 3 truncation values under the control law given in [16], which amounts to 15 more parameters than when only Gaussian distributions are considered. Nevertheless, Gaussian distributions (and even Gaussian Mixture Models) are unable to represent distributions with discontinuities which happens when a the control law exhibits a**

deadband. There is a need to know which is the best stochastic representation of each voltage node to provide a trade-off between accuracy and complexity.

The nature of a node voltage distribution is related to the distance of a node to a piecewise affine controlled DG. A heuristic method is proposed (flowchart of Fig.4) which selects, using standard conditions - whether a node voltage should a priori exhibit a Gaussian or a truncated sum of Gaussian distribution. A Monte Carlo method based on the Newton Raphson algorithm is used only once in the selection process. However, the optimization method presented in this paper and described in section III.C is not a Monte-Carlo method.

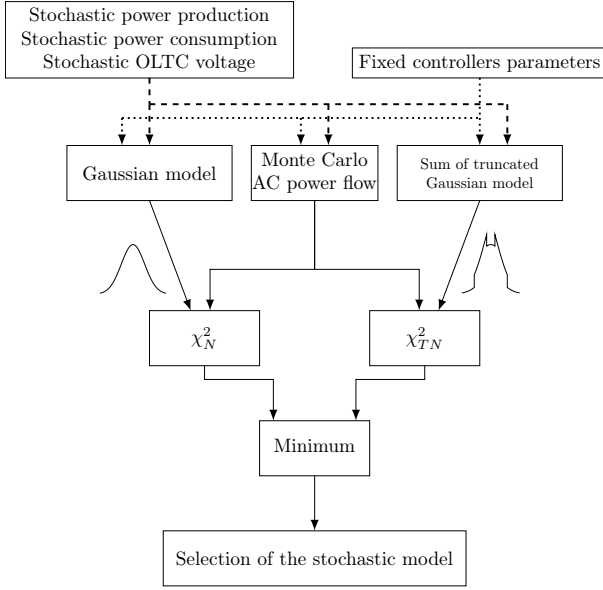


Fig. 4. Flowchart of the selection algorithm

First, the controllers parameters are fixed at standard values obtained by tuning local DG voltages. Then, by feeding the input powers and the OLTC voltage to a nonlinear model of the grid, nodes voltages PDFs are computed using Monte Carlo Simulations. Then, for each node, a Gaussian approximation and a sum of truncated Gaussian approximation of the voltage PDF are computed. For each node, the voltage interval is discretized with  $N$  values (e.g. in the interval  $[0.9; 1.1]$  pu, a step of  $0.002$  pu and  $N = 100$  can be selected). Eventually, Pearson's chi-squared test (21) is used to select the model which fits the node voltage PDF (obtained with Monte Carlo Simulations) best:

$$\chi^2 = \sum_{i=1}^N \frac{(p_i^{monte} - p_i^{fit})^2}{p_i^{monte}} \quad (21)$$

where  $p_i^{monte}$  is the expected frequency of type  $i$  obtained by Monte Carlo Simulations and  $p_i^{fit}$  is the frequency obtained by the Gaussian or the Piecewise Gaussian distribution. This test is able to compute a sum of relative error between the Monte Carlo Simulations and either a Gaussian law ( $\chi_N^2$ ), or a sum of truncated Gaussian laws ( $\chi_{TN}^2$ ). The numerical value of the test indicates the accuracy of the approximation in Proposition 1.

Once the selection procedure (which takes about ten minutes for the presented case study in section IV) is complete, the structure of every node voltage PDF is fixed, that is which PDFs should be represented by Gaussian variables (22) and which ones should be represented by sums of truncated variables (23). The choice between both types of model is obtained using a single set of standard control parameters. Then, the structure selected by this initialization procedure remains the same once and for all at each step in the confidence level optimization algorithm presented in section III.C.

$$\tilde{V}_i = \mathcal{N}(\mu_i^n, (\sigma_i^n)^2) \quad (22)$$

$$\tilde{V}_i = \sum_{j=1}^5 TN(\mu_i^j, (\sigma_i^j)^2, a_i^j, b_i^j) \quad (23)$$

### C. Definition of the optimization problem

In the previous section, it has been shown that voltage nodes can be represented by Gaussian or truncated Gaussian variables. The characteristics of their PDFs depend strongly on the piecewise affine controllers parameters, that is the breakpoints  $\gamma^j$ , levels  $Q^{0j}$  and the slopes  $\alpha_j$  of the piecewise functions. Hence, this model can be embedded in a confidence level optimization problem, for which the controllers parameters  $\gamma^j$ ,  $Q^{0j}$ ,  $\alpha^j$  and the reference voltage  $V_0^{ref}$  are the decision variables as shown in (24). A main objective is the maximization of the confidence levels  $\eta_i$  for which every voltage  $V_i$  remains within the specified range, in the case study  $[0.95; 1.05]$  pu. That is, one wants to provide a maximum level of service to the user. It is impossible to find a set of control parameters that give an optimal value for each individual confidence level, because of the strong coupling between the voltages and all control parameters, as shown in equation (20). Among all confidence levels, one should consider the worst one  $\eta_{worst}$  and try to maximize it. An alternative which was found to be more easily algorithmically tractable is to maximize the sum of all confidence levels, that is to minimize the occurrence of faulty situations, as shown in e.g. [26]. It is also sought to maximize the confidence level  $\lambda_i$  for which the DG powers of the node  $i$  remain within prescribed PQ domains. When the confidence levels are very high, secondary objectives are the reduction of the voltage variances ( $Var(\tilde{V}_i)$ ) and the DGs efforts ( $|\frac{\tilde{Q}_i^p}{P_i^N}|$ ). These objectives are scaled with weights  $w_V$  and  $w_Q$ . The means, variances, PDFs, CDFs and confidence levels of nodes voltages and DGs powers are computed using (11) to (20). They are not approximated and do not require multiple simulations. The objective function is given in the equation (24).

$$\begin{aligned} \max_{\alpha, \beta, Q^0, V_0^{ref}} w_\eta \min_{i=[0;n]} \eta_i + w_\lambda \min_{i=[0;n]} \lambda_i \\ - \frac{w_V}{n} \sum_{i=0}^n Var(\tilde{V}_i) - \frac{w_Q}{m} \sum_{i=0}^n \left| \frac{\tilde{Q}_i^p}{P_i^N} \right| \quad (24) \end{aligned}$$

Note that the decisions variables in equation (24)  $\alpha, \beta, Q^0$  are the affine, piecewise affine and OLTC control parameters. In addition to the objective functions, some technical or contractual constraints should be respected: There is a minimum



probability that the PQ powers remain in the prescribed PQ domain, that is the confidence level of the DG node  $g$   $\lambda_g$  should exceed a prescribed value  $\lambda_s$  as displayed in (25a). A well-designed network should never endure overcurrents. For all lines, the probability  $\delta_l$  that the conductor current  $I_l$  does not exceed the maximum bound  $I_{max}$  should be less than a prescribed value  $\delta_s$  (25b). The OLTC voltage reference  $V_0^{ref}$  should also remain within a prescribed interval (25c). The weights  $w_V, w_Q$  are normalized which allows for scale-up with respect to the size of the grid. Equations (25d) state that the outer intervals slopes of the piecewise affine control structure are set to zero to prevent DGs PQ powers to leave the contractual PQ diagram (e.g. if  $|\frac{\tilde{Q}_g^p}{P_g^N}|$  does not exceed  $-0.35$  or  $0.4$ , which are the bounds of the contractual PQ diagram). The central slope is enforced to zero which avoids to call for unnecessary actuation of the DGs reactive powers for low voltage variations (25d). Finally, for the interval  $j$ , the slopes  $\alpha_g^j$  of the industrial piecewise affine controller with 5 segments are bounded to keep the stability of the closed-loop system [27] (equation (25e)).

$$\lambda_g > \lambda_s \quad \forall DGs \quad (25a)$$

$$\delta_l > \delta_s \quad \forall conductors \quad (25b)$$

$$V_0^{ref} \in [V_0^{min}; V_0^{max}] \quad (25c)$$

$$\alpha_g^1 = 0 \quad \alpha_g^3 = 0 \quad \alpha_g^5 = 0 \quad (25d)$$

$$|\alpha_g^i| < \alpha_{max} \quad (25e)$$

The voltage  $\tilde{V}_i$  is a sum of truncated Gaussian variables which allows to deal with discontinuities and is characterized by :

$$F_{\tilde{V}_i}(x) = \begin{cases} \Phi\left(\frac{x-\mu_i^1}{\sigma_i^1}\right) & \text{if } x \in ]-\infty; b_i^1] \\ \Phi\left(\frac{x-\mu_i^2}{\sigma_i^2}\right) & \text{if } x \in ]a_i^2; b_i^2] \\ \Phi\left(\frac{x-\mu_i^3}{\sigma_i^3}\right) & \text{if } x \in ]a_i^3; b_i^3] \\ \Phi\left(\frac{x-\mu_i^4}{\sigma_i^4}\right) & \text{if } x \in ]a_i^4; b_i^4] \\ \Phi\left(\frac{x-\mu_i^5}{\sigma_i^5}\right) & \text{if } x \in ]a_i^5; +\infty[ \end{cases} \quad (26)$$

The confidence level  $\eta_i$  that the voltage  $\tilde{V}_i$  remain within  $[V_{min}; V_{max}]$  is given by  $\eta_i = F_{\tilde{V}_i}(V_{max}) - F_{\tilde{V}_i}(V_{min})$

Knowing the nature of the distributions allows to boil down the complex behavior to a few parameters (variances, means, truncation values) and to compute straightforwardly the optimization objective (confidence levels, etc.). This is a main advantage over a trial and error procedure such as the Monte-Carlo method. For example, consider a real distribution grid with 4000 nodes, 100 parameters to tune and 1000 samples are taken for each Monte Carlo simulation. Let us assume that the 4000 densities of probability are obtained within 500 seconds on a standard computer, and that the algorithm converges in 20 iterations (steps). If we use a brute force algorithm, the total computational time will amount to 2000000 seconds, that is more than 500 hours. Even with an improved optimization code, and a reduction of the computational cost by 100, the optimization problem would be solved in 5 hours. This method is able to reach an optimal solution within 10 minutes, which

allows for hourly updates. It is possible to embed losses in the objective function, which is done generally, however, at the design stage as explained in [28].

#### IV. APPLICATION OF CONFIDENCE LEVEL OPTIMIZATION TO A REAL DISTRIBUTION GRID

##### A. Description of the case study

The optimization problem (24) s.t. (25) is applied to a grid based on a real distribution network. The grid contains 3441 nodes, 690 loads, 21 generators (mainly PV), which are distributed on 27 feeders. The maximal consumption of loads is 84.1 MW and 38 MVar. The nominal power of all generators is 29.5 MW. Only one DG per mixed feeder is equipped with a piecewise affine controller. Other DGs reactive power controllers are affine. There are 7 feeders equipped with a piecewise affine controller, and 14 DGs equipped with an affine controller. This distribution grid is real so it is designed to avoid overvoltages. However, in the future, new distributed generators could be added to an existing grid without other topology and hardware modification. In the case study, one check whether two additional DG with an active power 3 MW can be added to mixed feeders. The idea is to tune all DGs reactive power controllers and find the appropriate OLTC voltage to keep voltages and powers in the prescribed domains. The result on the whole distribution is too long and cannot be detailed, but can be handled in less than 10 minutes by the optimization algorithm. The mixed feeder presented in Fig.5 is relevant to illustrate the proposed method.

The tuning is performed using a realistic and critical operation, which occurs typically at the beginning of the afternoon in summer. As load and production rates are respectively 30 % and 80 %, working conditions create situations for which voltages are close to the upper bounds. The characteristics of forecasting errors can be inferred from a measurement data base and are summarized in Table I, and load spreading uncertainty is considered in the study.

TABLE I. UNCERTAINTIES STANDARD DEVIATIONS

Uncertainty (in % of nominal or reference power)	Standard deviation
Aggregated load forecast uncertainty	3.45 %
Load spreading uncertainty	50 %
Production forecast uncertainty (photovoltaic energy)	17.16 %
OLTC uncertainty	0.005 pu

##### B. Results and discussion

Proposition 1 has shown that all voltages can be modeled by either Gaussian variables or sums of truncated Gaussian variables. The initialization stage selects the stochastic model of the voltages nodes. The distribution of the models in one of the 27 feeders, shown in Fig.5, is detailed.

The nodes voltages close to the DG (from node 101 to the feeder end) can be modeled by sum of truncated Gaussian variables. About 1/3 of nodes voltages distributions are approximated by piecewise Gaussian distributions and the

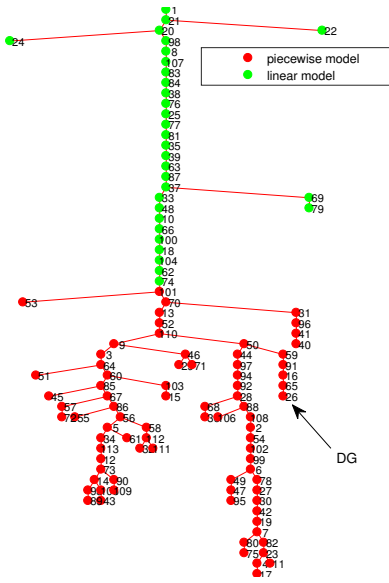


Fig. 5. Illustration of the mixed feeder and the stochastic model selected

remaining 2/3 can be represented by Gaussian distributions. The nature of the distribution changes between nodes 74 and 101. The DG equipped with a piecewise affine controller is located at node 26.

A confidence level optimization program is not a linear program, and no formal proof of convergence or convexity can be given when it involves piecewise affine functions. However, using a Monte Carlo method, the numerical convexity of the problem has been assessed. The optimization is applied to the whole grid, uses a classical interior point method of the routine `fmincon` [29] of Matlab 2016b dedicated to solve convex problems [29] and is performed on a PC with 2.8 GHz Intel Core i7 and 16 GB RAM. The constraints settings are  $\lambda_s = \delta_s = 0.95$ ,  $V_0^{min} = 1.02 pu$ ,  $V_0^{max} = 1.04 pu$ ,  $\alpha_{max} = 15 pu/pu$ . The optimal solution (which verifies the constraints (25)) is computed within 10 minutes on a standard computer which allows, if necessary, an hourly update.

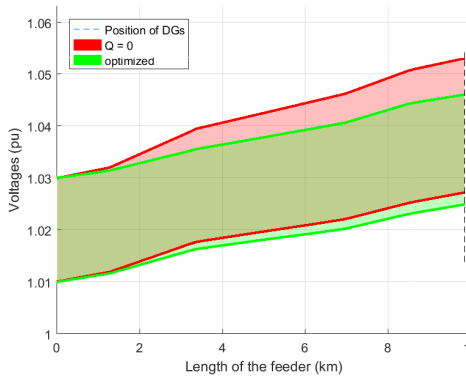


Fig. 6. Optimized possible voltages along the feeder

Results related to the feeder shown in Fig.5 is detailed. A global view of the possible voltages along the feeder is shown in Fig.6. These results are obtained with the AC power flow method with Monte Carlo Simulations used as the reference method. The filled area represents 95 % of the

voltages which lie within 2 standard deviations of the mean, in green with optimized control, and red without reactive power. This figure demonstrates that nodes voltages are kept in the domain  $[0.95; 1.05] pu$ , and that voltage variances are reduced, specifically when close to the DG. The optimization algorithm sets the OLTC reference voltage to  $1.02 pu$  which is the lowest bound allowed. It is consistent with the fact that under this operating point, the distribution grid endures high voltage problems. The DG at the feeder end (node 26) has a voltage mean of  $1.035 pu$  and standard deviation of  $0.05 pu$ , which can be compared with the  $1.04 pu$  mean and  $0.06 pu$  standard deviation of the uncontrolled voltage.

The piecewise affine function controlling the DG reactive power and the voltage of the node connected to the DG are both presented in Fig.7. One can see that the controller is mainly activated in one interval (the decreasing segment between  $1.028 pu$  and  $1.043 pu$ ). The optimized value of the segment slope is  $-13.5 pu/pu$  which is close to the the lower bound, thereby allowing to decrease the variance. The last segment after  $1.043 pu$  enforces the reactive power rate to a value of  $-0.28 pu$ . Fig.7 shows that this value corresponds to a voltage bound of  $1.05 pu$ .

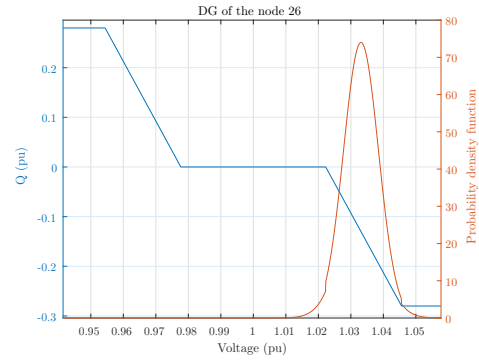


Fig. 7. The optimized piecewise affine function with its voltage PDF

The reduction of the DGs efforts is a very important result of the optimization. Decreasing DGs efforts improves DGs lifetime, and reduces maintenance operations. Fig.8 shows the PDF of the reactive power which can be split into three parts. These parts are outer bounds with two fixed values ( $-0.28 pu$  and  $0 pu$ ) and an intermediate part which is a truncated Gaussian variable with a mean value of  $-0.15 pu$ .

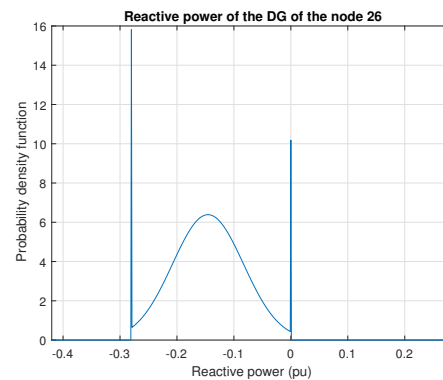


Fig. 8. The reactive power PDF

The optimized DG effort is  $\mu_Q^{optim} = 0.14 pu$ , which can be compared to the same DG effort obtained with the French parameters of the law  $Q = f(V)$  [30]. At the same operating point, these parameters impose the DG effort to be  $\mu_Q^{french} = 0.1606 pu$ . This comparison shows that the optimization can save 10% DG effort. This gain is the result of the short-term optimization. The DG effort can be optimized in the range  $[0.06; 0.16] pu$  and the node 26 voltage standard deviation can be optimized in the range  $[0.005; 0.006] pu$ . All the subparts of the objective function (24) are conflicting and the weighting factors  $w_\lambda, w_\eta, w_V, w_Q$  can be selected by finding a Pareto optimum. A Pareto frontier between the mean of DG efforts and the maximum risk level is given in Fig.9. Using a Pareto barrier for the four weighting factors, one obtains  $w_\eta = w_\lambda = 0.9995, w_V = 1, w_Q = 0.0005$ . When the priority is given to only DGs efforts reduction, a value of  $\mu_Q^{optim} = 0.06 pu$  can be obtained, dividing these efforts by 50 % .

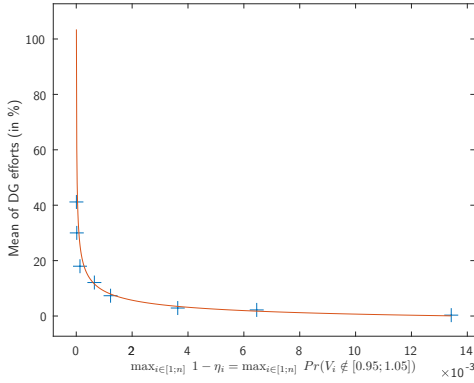


Fig. 9. Pareto frontier between the mean of DG efforts and the risk level  $1 - \min_{i \in [1;n]}(\eta_i)$

Whereas the tuning method needs a distribution of the forecast errors in a time window (i.e. probabilities), their time-profile is not required as for real-time control. Contrary to advanced real-time control (e.g. predictive control), the method can be applied with the current communication and actuation technologies. The price to be paid is reasonable and consists of sending periodically (say on an hourly basis) the stochastic behavior of the production and consumption forecasts to a centralized supervisor, which, in turn, after performing a confidence level optimization, should communicate periodically (on the same time basis) their new control parameter to each DER. Note however that once this is done, the DERs operate in a fully decentralized mode. In France, this could be done using a device called DEIE [31].

## V. CONCLUSION

The paper addresses a centralized optimization of the controllers settings in a distribution grid with a stochastic representation of renewable productions and consumptions. The controllers actuate the OLTC and the DGs reactive powers and enforce both the nodes voltages to remain within specified bounds and the DG powers to stay in a prescribed PQ domain. DGs reactive power controllers have a droop-like structure

and may embed a dead-band term which is used to decrease unnecessary actuation.

The proposed stochastic model uses Gaussian variables or sums of truncated Gaussian variables to represent nodes voltages and DGs reactive powers. Their characteristics (mean, variance, confidence level) can be inferred from the stochastic model and control parameters.

The suggested optimization algorithm finds the DG piecewise affine controller parameters (levels and breakpoints) and the OLTC voltage reference which minimize a weighted sum of voltage variances, confidence levels and DG efforts. The proposed method has been applied on the model of a real distribution network. The DGs efforts are cut by half while nodes voltages and DG powers remain within the prescribed domains. It is possible to extend the results of Proposition 1 to the case where several piecewise affine controllers can be found in a feeder. In this case, the stochastic truncations from several feeders will propagate along the lines, and the interactions between the piecewise affine controllers must be considered. Intuitively, one can consider that results from Proposition 1 are still relevant when two DGs are close and can be aggregated or when they are far with a weak coupling. The modelling problem has been addressed with an algorithm similar to the selection procedure of section III.B in [32]. Future works will design a daily planning of grid operations considering infrequent and asynchronous updates of the DG controllers. The main issue will be to predict possible critical voltage problems and trigger an update of voltage controllers parameters.

## APPENDIX

### PROPERTIES OF TRUNCATED GAUSSIAN VARIABLES

A truncated Gaussian variable is a Gaussian variable which is truncated in an interval. Consider the Gaussian variable  $\tilde{X} \sim \mathcal{N}(\mu, \sigma^2)$ , the truncated Gaussian variable  $\tilde{Y}$  of the equation (27) is based on  $\tilde{X}$  and is truncated in the interval  $[a; b]$ . The PDF is given by (28).

$$\tilde{Y} = Pr(\tilde{X} | a < \tilde{X} < b) \sim TN(\mu, \sigma^2, a, b) \quad (27)$$

$$f(x; \mu, \sigma, a, b) = \begin{cases} \frac{\phi(\frac{x-\mu}{\sigma})}{\sigma(\Phi(\frac{b-\mu}{\sigma}) - \Phi(\frac{a-\mu}{\sigma}))} & \text{for } a \leq x \leq b \\ 0 & \text{otherwise} \end{cases} \quad (28)$$

where  $\phi(x) = \frac{1}{\sqrt{2\pi}} e^{-\frac{1}{2}x^2}$  the standard Gaussian PDF and  $\Phi(x) = \int_{-\infty}^x \phi(t) dt = \int_{-\infty}^x \frac{1}{\sqrt{2\pi}} e^{-\frac{1}{2}t^2} dt$  is the standard Gaussian Cumulative Distribution Function (CDF).

## REFERENCES

- [1] P. P. Barker and R. W. D. Mello, "Determining the impact of distributed generation on power systems. i. radial distribution systems," in *2000 Power Engineering Society Summer Meeting*, 2000, pp. 1645–1656.
- [2] A. Zidan, M. Khairalla, A. M. Abdrabou, T. Khalifa, K. Shaban, A. Abdrabou, R. E. Shatshat, and A. M. Gaouda, "Fault detection, isolation, and service restoration in distribution systems: State-of-the-art and future trends," *IEEE Trans. Smart Grid*, vol. 8, no. 5, pp. 2170–2185, 2017.
- [3] E. Dall'Anese, K. Baker, and T. Summers, "Chance-constrained ac optimal power flow for distribution systems with renewables," *IEEE Trans. Power Systems*, vol. 32, no. 5, pp. 3427–3438, 2017.

- [4] J. Morin, F. Colas, J. Dieulot, S. Grenard, and X. Guillaud, "Embedding oltc nonlinearities in predictive volt var control for active distribution networks," *Electric Power Systems Research*, vol. 143, pp. 225–234, 2017.
- [5] D. K. Molzahn, F. Dorfler, H. Sandberg, S. H. Low, S. Chakrabarti, R. Baldick, and J. Lavaei, "A survey of distributed optimization and control algorithms for electric power systems," *IEEE Trans. Smart Grid*, vol. 8, no. 6, pp. 2941–2962, 2017.
- [6] W. Powell and S. Meisel, "Tutorial on stochastic optimization in energy I: Modeling and policies," *IEEE Trans. on Power Systems*, vol. 31, pp. 1459–1467, 2016.
- [7] C. Rahmann, A. Heinemann, and R. Torres, "Quantifying operating reserves with wind power: towards probabilisticdynamic approaches," *IET Generation, Transmission and Distribution*, vol. 10, pp. 366–373, 2016.
- [8] P. Beraldi, A. Violi, M. Bruni, and G. Carrozzino, "A probabilistically constrained approach for the energy procurement problem," *Energies*, vol. 10, p. 2179, 2017.
- [9] W. van Ackooij, R. Henrion, A. Miller, and R. Zorghi, "Joint chance constrained programming for hydro reservoir management," *Optimization and Engineering*, vol. 15, pp. 509–531, 2014.
- [10] K. Baker, E. Dall'Anese, and T. Summers, "Distribution-agnostic stochastic optimal power flow for distribution grids," in *2016 North American Power Symposium (NAPS)*, 2016, pp. 1–6.
- [11] W. Yuan, J. Wang, F. Qiu, C. Chen, C. Kang, and B. Zeng, "Robust optimization-based resilient distribution network planning against natural disasters," *IEEE Trans. Smart Grid*, vol. 7, no. 6, pp. 2817–2826, 2016.
- [12] K. Baker, A. Bernstein, E. Dall'Anese, and C. Zhao, "Network-cognizant voltage droop control for distribution grids," *IEEE Trans. Power Systems*, vol. PP, no. 99, pp. 1–1, 2017.
- [13] S. Bolognani and S. Zampieri, "On the Existence and Linear Approximation of the Power Flow Solution in Power Distribution Networks," *IEEE Trans. Power Systems*, vol. 31, no. 1, pp. 163–172, 2016.
- [14] S. Shojaabadi, S. Abapour, M. Abapour, and A. Nahavandi, "Optimal planning of plug-in hybrid electric vehicle charging station in distribution network considering demand response programs and uncertainties," *IET Generation, Transmission Distribution*, vol. 10, no. 13, pp. 3330–3340, 2016.
- [15] S. Huang, Q. Wu, J. Wang, and H. Zhao, "A sufficient condition on convex relaxation of ac optimal power flow in distribution networks," *IEEE Trans. Power Systems*, vol. 32, no. 2, pp. 1359–1368, 2017.
- [16] L. Gan, N. Li, U. Topcu, and S. H. Low, "Exact convex relaxation of optimal power flow in radial networks," *IEEE Trans. Automatic Control*, vol. 60, no. 1, pp. 72–87, 2015.
- [17] S. Weckx and J. Driesen, "Optimal local reactive power control by pv inverters," *IEEE Trans. Sustainable Energy*, vol. 7, no. 4, pp. 1624–1633, 2016.
- [18] J. Xie, T. Hong, T. Laing, and C. Kang, "On normality assumption in residual simulation for probabilistic load forecasting," *IEEE Trans. on Smart Grid*, vol. 8, no. 3, pp. 1046–1053, 2017.
- [19] P. Kou, D. Liang, L. Gao, and F. Gao, "Stochastic coordination of plug-in electric vehicles and wind turbines in microgrid: A model predictive control approach," *IEEE Trans. Smart Grid*, vol. 7, no. 3, pp. 1537–1551, 2016.
- [20] Y. Chen, A. Busic, and S. Meyn, "Estimation and control of quality of service in demand dispatch," *IEEE Trans. Smart Grid*, vol. PP, no. 99, pp. 1–1, 2017.
- [21] C. Wang, A. Bernstein, J. Y. L. Boudec, and M. Paolone, "Explicit conditions on existence and uniqueness of load-flow solutions in distribution networks," *IEEE Trans. Smart Grid*, vol. PP, no. 99, pp. 1–1, 2017.
- [22] J. Buire, X. Guillaud, F. Colas, J. Dieulot, and L. De Alvaro, "Combination of linear power flow tools for voltages and power estimation on mv networks," in *24th International Conference and Exhibition on Electricity Distribution, CIRED 2017*, 2017, pp. 1–4.
- [23] P. Pinson, H. Madsen, H. A. Nielsen, G. Papaefthymiou, and B. Klckl, "From probabilistic forecasts to statistical scenarios of short-term wind power production," *Wind Energy*, vol. 12, pp. 51–62, 2009.
- [24] M. Cosson, H. Gueguen, P. Haessig, D. Dumur, C. Maniu, V. Gabrion, and G. Malarange, "Stability criterion for voltage stability study of distributed generators," in *Workshop on Control of Transmission and Distribution Smart Grids (CTDSG)*, 2016, pp. 1–13.
- [25] M. L. Eaton, *Chapter 3: The normal distribution on a vector space*, ser. Lecture Notes-Monograph Series. Beachwood, Ohio, USA: Institute of Mathematical Statistics, 2007, vol. 53.
- [26] R. W. Freund and F. Jarre, "Solving the sum-of-ratios problem by an interior-point method," *Journal of Global Optimization*, vol. 19, pp. 83–102, 2001.
- [27] M. Cosson, H. Gueguen, D. Dumur, C. S. Maniu, V. Gabrion, and G. Malarange, "Voltage stability of distributed generators by means of discrete abstraction," in *2015 IEEE Conference on Control Applications (CCA)*, 2015, pp. 195–200.
- [28] G. Valverde and T. V. Cutsem, "Model predictive control of voltages in active distribution networks," *IEEE Trans. Smart Grid*, vol. 4, pp. 2152–2161, 2013.
- [29] R. H. Byrd, J. C. Gilbert, and J. Nocedal, "A trust region method based on interior point techniques for nonlinear programming," *Mathematical Programming*, vol. 89, no. 1, pp. 149–185, 2000.
- [30] "Modalités du contrôle de performances des Installations de Production raccordées en haute tension (HTA) au Réseau Public de Distribution géré par Enedis," p.5. [Online]. Available: [http://www.enedis.fr/sites/default/files/Enedis-NOI-RES\\_60E.pdf](http://www.enedis.fr/sites/default/files/Enedis-NOI-RES_60E.pdf), accessed on: Aug 31, 2018.
- [31] G. Foggia, A. Neto, and A. Michiorri, "Coordinated control of dispersed battery energy storage systems for services to network operators," in *23th International Conference and Exhibition on Electricity Distribution, CIRED*, 2015.
- [32] J. Buire, X. Guillaud, F. Colas, J. Dieulot, and L. De Alvaro, "Stochastic power flow of distribution networks including dispersed generation system," in *IEEE PES Innovative Smart Grid Technologies Conference, ISGT Europe, Sarajevo*, 2018, pp. 1–6.